

2001

# A Method of Non-Data-Aided Carrier Recovery with Modulation Identification

Robert H. Morelos-Zaragoza

*SONY Computer Science Laboratories, Inc.*, robert.morelos-zaragoza@sjsu.edu

Kenta Umebayashi

*Yokohama National University*

Ryuji Kohno

*Yokohama National University*

Follow this and additional works at: [http://scholarworks.sjsu.edu/ee\\_pub](http://scholarworks.sjsu.edu/ee_pub)

 Part of the [Electrical and Computer Engineering Commons](#)

---

## Recommended Citation

Robert H. Morelos-Zaragoza, Kenta Umebayashi, and Ryuji Kohno. "A Method of Non-Data-Aided Carrier Recovery with Modulation Identification" *Faculty Publications* (2001): 3375-3379. doi:10.1109/GLOCOM.2001.966311

This Article is brought to you for free and open access by the Electrical Engineering at SJSU ScholarWorks. It has been accepted for inclusion in Faculty Publications by an authorized administrator of SJSU ScholarWorks. For more information, please contact [scholarworks@sjsu.edu](mailto:scholarworks@sjsu.edu).

# A Method of Non-Data-Aided Carrier Recovery with Modulation Identification

Robert H. Morelos-Zaragoza  
 SONY Computer Science Laboratories, Inc.  
 3-14-13 Higashigotanda, Shinagawa-ku  
 Tokyo 141-0022 Japan

Kenta Umebayashi and Ryuji Kohno  
 Yokohama Natl. University  
 79-5 Tokiwadai, Hodogaya  
 Yokohama 240-8501 Japan

*Abstract*—A non-data aided carrier recovery technique using modulation format identification is proposed. This technique can also be interpreted as a modulation identification method that is robust against static phase and frequency offsets. The performance of the proposed technique is studied and analytical expressions derived for the mean acquisition time to detect lock in the cases of  $M$ -PSK,  $M = 2, 4, 8$ , and 16-QAM modulation, with respect to frequency offset and signal-to-noise ratio. The results are verified with Monte Carlo simulations. The main advantage of the proposed method lies in its simpler implementation and faster lock detection, when compared to conventional methods.

## I. INTRODUCTION

In wireless communications systems, the presence of multiple standards and the need to use denser signal constellations to support the demand of ever higher data rates require digital receivers that can operate with multiple modulations. To speed up the carrier acquisition process, as well as to reduce system overhead, it is of practical interest to design receivers able to identify the format of the incoming signals. In [1], a technique based on fourth-order cumulants was proposed to identify modulation formats, and shown to be robust against carrier frequency and phase offsets. A method of modulation identification is proposed here that can also handle frequency and phase offsets, through the use of a conventional digital phase-locked loop (PLL) [2] and a modulation identification technique previously proposed in [3]. The parameters of the PLL, such as phase error detector (PED) characteristics, are reconfigured based on the information produced by a bank of phase-lock detectors (PLD) and an identification (ID) logic. This PLL is referred to as a *multiple-mode digital PLL*. In this paper, the focus is on carrier recovery and thus perfect symbol timing is assumed. Under frequency and phase offsets, the identification logic needs to be designed in such a way that, even when the incoming constellations are rotating, their modulation format is successfully identified. To achieve this, the ID logic of [3] was modified by adding more hit counters associated with specific sectors within lock areas. The proposed technique does not exclude the use of other modulation ID approaches, such as that proposed in [1]. Therefore, a main contribution of this paper is that information of the modulation format being received can be used to *reconfigure* the parameters and even the structure of the synchronization circuits or algorithms, e.g., from non data aided to decision directed. This is a very desirable feature in a software radio receiver. Moreover, the proposed multiple-mode carrier recovery scheme has less complexity than the use of cumulants [1].

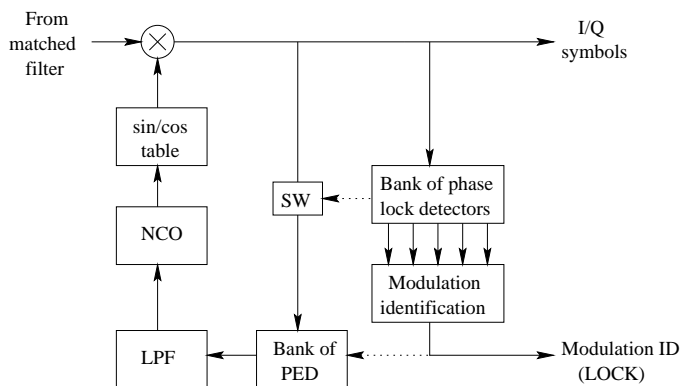


Fig. 1. Block diagram of a multiple-mode digital PLL

### A. Carrier recovery aided by modulation identification

A simplified block diagram of the proposed system is shown in Fig.1. In the figure,  $SW$  denotes a switch to open or close the carrier recovery loop. Initially, switch  $SW$  is open and the incoming signal symbols rotate at a speed which is given by the mismatch or offset — denoted here by  $\Delta f$  — between the frequencies of the received carrier signal,  $f_c$ , and the local oscillator signal,  $f_{LO}$ . Assume that  $\Delta f$  is small compared to the symbol rate,  $R_s$ , so that the received signal lies within the capture range of the digital PLL. This condition is equivalent to  $\Delta f T_s \ll 1$ , where  $T_s = 1/R_s$  is the symbol interval. It can be argued that in high-speed wireless communications systems this is a reasonable assumption. Equivalently, the results of this work apply to single-carrier narrow-band wireless communications systems employing multiple digital linear modulations. Also, perfectly equalized (and ideally timed) received signals are considered, so that the only perturbation is caused by additive noise.

More precisely, in complex baseband representation, at the  $n$ -th symbol interval  $t \in [(n-1)T_s, nT_s]$ , let  $s_n = b_n e^{j\theta_n}$  denote a transmitted constellation point, where  $T_s$  denotes the symbol duration. Then, in the absence of carrier frequency or phase offsets, the corresponding received symbol is given by

$$r_n = s_n + g_n,$$

where  $g_n$  are samples of a complex zero-mean additive white Gaussian noise (AWGN) process with power spectral density

$N_0$ . It is assumed, without loss of generality, that a frequency offset  $\Delta f = |f_c - f_{LO}|$  exists between carrier and local signals. Then the received symbol can be expressed as

$$r_n = s_n e^{j2\pi n \Delta f T_s} + g'_n = b_n e^{j(\theta_n + n2\pi \Delta f T_s)} + g'_n, \quad (1)$$

where  $g'_n$  is a sample of an AWGN process, with the same statistics as  $g_n$ . Let the *normalized frequency offset* be  $\Delta f T_s$ . From equation (1) above, with respect to the phases  $\theta_n$ , the received points  $r_n$  rotate at an angular speed equal to  $2\pi \Delta f$  radians every  $T_s$  seconds. With this setting, it becomes evident that the purpose of the carrier recovery circuit or algorithm is to estimate the angular speed of the received points and to apply a rotation to them, in the opposite way, such that the points output by the carrier recovery subsystem are “de-rotated” and close to their ideal positions.

### B. A multiple-mode digital PLL

The digital PLL considered in this paper is of the conventional type, with a proportional-and-integral low pass filter (LPF). With reference to the block diagram of the multiple-mode digital PLL shown in Fig. 1, the input to the LPF is the phase error produced by the PED. The output of the LPF is then fed to a numerically controlled oscillator (NCO), to output the phases of complex baseband symbols rotating at a frequency approximately equal to the negative of the frequency offset (or opposite way with reference to the received symbols.) The main difference with respect to a conventional type PLL is the presence of a bank of PLD and a modulation ID logic, which are used to select the phase-error detectors that correspond to the received digital modulation formats.

It is assumed that the digital PLL contains a bank of four PEDs, for each of the following digital modulations: BPSK, QPSK, 8PSK and 16QAM. The constellations are normalized to unit energy. The modulation ID output is used either to select one out of the four PEDs, in correspondence to the identified modulation, or to keep the loop open, if no modulation format has been recognized yet.

The output of the identification logic is an integer that represents the number of bits per constellation symbol. That is, integers 1, 2, 3 and 4 are used to identify BPSK, QPSK, 8PSK and 16QAM, respectively. If no modulation format is recognized, a zero value is output by the logic.

## II. MODULATION IDENTIFICATION UNDER FREQUENCY/STATIC PHASE OFFSETS

Under frequency/static phase offsets, the modulation identification logic introduced in [3] exhibits false locks or misidentifies often. In order to prevent the ID logic from incorrectly identifying a rotated constellation, additional lock area counters are needed. A threshold value  $N_T$  is associated with each lock area counter. At the end of an observation window, i.e., when the number of symbols reaches the observation window length

$N$ , the value of the counter  $N_C$  is compared to the threshold  $N_T$ . Lock condition is declared, or lock flag set to ‘1’, whenever  $N_C > N_T$ .

To operate under frequency offsets, additional counters and corresponding thresholds were introduced in the identification logic. In the current multiple-mode digital receiver, the observation period equals  $N = 50$  with global thresholds set to  $N_T = 27$ .

Note that a BPSK constellation rotated by  $\pi/4$  radians “looks” like a QPSK constellation, in the sense that the majority of the received points lie in the QPSK area. However, note that most of these hits occur in two *opposite* sectors.

Consequently, two additional counters were incorporated in the QPSK identification portion of the ID logic — with thresholds equal to 0 in the MATLAB simulations reported later in the paper.

The additional counters are associated with two adjacent sectors, corresponding to constellation points at phases  $\theta$  and  $\theta + \pi/2$ , where  $\theta$  can be any of four possible values:  $\{\pi/4, 3\pi/4, -3\pi/4, -\pi/4\}$ . The value  $\theta = -3\pi/4$  was selected arbitrarily.

Similarly, for the identification of 8PSK modulation, two additional counters — with thresholds equal to 0 — were used in two adjacent sectors. In the case of 16-QAM modulation, one counter was introduced to count the number of hits in an inner sector, in addition to the global counter — and the threshold for this inner sector counter was set to 2 in simulations and experiments.

Also, the case of a *static* (i.e., independent of time) phase offset needs to be considered. In the proposed carrier recovery technique, a time-out mechanism is used. If after an adjustable time-out period, no lock has been detected, a small frequency offset is introduced in the loop. We note that a carrier loop including this functionality is shown in [2], p. 550, under the name *acquisition control*.

Results from computer simulations and experiments in a software-defined radio (SDR) platform indicate that this is an effective way to remove a static phase offset, provided that the *scanning frequency offset* (SFO) is small enough so as to not make any frequency offset worse. An observation window of  $N = 50$  symbols and a time-out period equal to  $20N = 1000$  symbols was used. When the receiver is in scanning mode, the SFO is set to a small value equal to  $\pi/4096$  radians every  $10N = 500$  symbols. The acquisition time in the case of a static phase offset is thus in the order of thousands of symbols. This is acceptable, since a static offset will most likely occur during the receiver’s power-up stage or whenever the received modulation format changes.

## III. PERFORMANCE ANALYSIS

It is important to observe that there is a delicate balance between the frequency offset  $\Delta f T_s$ , the signal-to-noise ratio per symbol,  $E_s/N_0$ , and the size of the observation window,  $N$ . At low  $E_s/N_0$ , the value of  $N$  should be set as high as possible, as

TABLE I  
MAXIMUM FREQUENCY OFFSET WITH A THRESHOLD OF 27 SYMBOLS

MOD	$\Phi$ (deg)	$(\Delta f T_s)_{\max}$
BPSK	90	0.00926
QPSK	45	0.00463
8PSK	22.5	0.00231
16QAM	17.8	0.00183

done in [3], in order to average out the effects of additive noise. At the same time, however,  $N$  is limited by the value of  $\Delta f T_s$ . That is, if  $\Delta f T_s$  is relatively large, then  $N$  needs to be small enough so that most of the signal points lie in the lock area.

#### A. Maximum frequency offset

In this section, the maximum frequency offset for which the signals can be recovered is estimated, under the assumption that no AWGN is added to the received signals. Formally, consider a lock area with an angular range  $\Phi$ . Note that the phase increment between symbols equals  $2\pi\Delta f T_s$  radians. Consequently, the maximum normalized frequency offset is given by

$$(\Delta f T_s)_{\max} = \left( \frac{\Delta f}{R_s} \right)_{\max} = \frac{\Phi}{2\pi N_T}, \quad (2)$$

where  $T_s = 1/R_s$  is the symbol interval and  $N_T$  is the counter threshold. It follows that the maximum frequency offset sets an upper bound on the value of  $N_T$ . The larger the value of  $(\Delta f T_s)_{\max}$ , the smaller the value of  $N_T$ , and viceversa. Table I shows the values of  $(\Delta f T_s)_{\max}$  with a threshold  $N_T = 27$ , for the four modulations of interest in this paper.

The angular range for 16QAM is approximated by the worst case (in the absence of noise), which is given by the lock area corresponding to an outer (or corner) point in the constellation. This means that 16-QAM constellation can be recovered even in cases of a slightly higher  $\Delta f$ .

#### B. Probability of lock detection under frequency offsets

In this section, the probability of lock detection of each PLD is analyzed under the assumptions of perfect symbol timing and equalization (i.e., no residual interference due to multipath fading). The results in this section will be used to estimate the mean acquisition time of the proposed NDA recovery scheme.

Let  $\Delta\theta = 2\pi\Delta f T_s$  and consider a received symbol  $s_0$  at the beginning of an observation window of length  $N$  symbols. Let  $\phi$  denote the phase of  $s_0$ . If  $|\Delta f| \neq 0$ , as mentioned above, subsequent symbols will “rotate” at a speed of  $\Delta\theta$  radians per symbol. Therefore, the  $i$ -th symbol within the observation window,  $0 \leq i < N$ , will experience a phase rotation equal to  $i\Delta\theta$  with respect to  $s_0$ . Recall that lock detection is successful if the number of received symbols inside the lock area is greater than a threshold value  $N_T$  over the observation window of length  $N$  symbols.

For clarity of presentation, a bound on the probability of lock detection is derived below for the case of BPSK modulation, as a function of the phase of the first received symbol  $s_0$ , the normalized frequency offset  $\Delta\theta$ , and the signal-to-noise ratio per symbol  $E_s/N_0$ . The probability that the  $i$ -th received symbol,  $s_i$ , lies inside the BPSK lock area, denoted  $\mathcal{L}$ , given that the initial symbol has a phase  $\phi$ , can be lower bounded as

$$\Pr\{s_i \in \mathcal{L} | \phi\} \triangleq p_i \geq 1 - \left[ Q \left( \cos(\phi + i\Delta\theta) \sqrt{\frac{E_s}{N_0}} \right) + Q \left( \sin(\phi + i\Delta\theta) \sqrt{\frac{E_s}{N_0}} \right) \right], \quad (3)$$

where  $Q(x)$  is the Gaussian  $Q$ -function.

The probability  $P_o(M, \phi)$  that  $M$  symbols lie outside of the lock area  $\mathcal{L}$ , given an initial phase  $\phi$ , is  $P_o(0, \phi) = \gamma$ , and

$$P_o(M, \phi) = \sum_{j=0}^{M-1} \left( \sum_{a_j=a_{j-1}+1}^{N-1-(M-1-j)} \gamma \prod_{\ell=1}^{M-1} q_{a_\ell} \right), \quad M \geq 1, \quad (4)$$

where  $a_{-1} \triangleq 0$ ,  $\gamma = \prod_{i=0}^{N-1} p_i$  is the probability that all the received symbols in the window are inside the lock area, and

$$q_{a_\ell} \triangleq \frac{(1 - p_{a_\ell})}{p_{a_\ell}}. \quad (5)$$

From Eqs. (3) to (5), the probability of lock, i.e., the probability that up to  $N - N_T$  symbols lie outside of region  $\mathcal{L}$ , given the initial phase  $\phi$ , is approximated as

$$\Pr\{\text{Lock} | \phi\} \approx \sum_{i=0}^{N-N_T} P_o(i, \phi). \quad (6)$$

Note that  $\Pr\{\text{Lock} | \phi\}$  is a random variable that depends on  $\phi$ . Integrating over the probability density function of the initial phase  $\phi$ , leads to the following expression for the probability of lock detection

$$\Pr\{\text{Lock}\} \approx \int_0^{2\pi} \sum_{i=0}^{N-N_T} P_o(i, \phi) p_\phi(\phi) d\phi. \quad (7)$$

Assuming a uniform distribution on the value of the initial phase  $\phi$ , expression (7) can be written as

$$\Pr\{\text{Lock}\} \approx \frac{1}{2\pi} \sum_{i=0}^{N-N_T} \int_0^{2\pi} P_o(i, \phi) d\phi. \quad (8)$$

The bound (8) was evaluated numerically (via Monte Carlo integration) and is plotted versus  $E_s/N_0$ , for several values of normalized frequency offset. A similar argument holds for QPSK and 8-PSK modulations. For details, the reader is referred to [4].

It should be pointed out that in the case of 16-QAM, the expression for  $p_i$  becomes more involved, as it depends on the particular type of symbol being received, i.e., inner, wall or corner.

Also note from the plots that, at high  $E_s/N_0$ , the probability of lock approaches a constant value greater than or equal to 0.5. The value of the constant can be computed for BPSK modulation, as follows:

Consider the case with no frequency offset,  $|\Delta f| = 0$ . Given a random initial phase  $\phi$  with uniform distribution in the range  $[0, 2\pi)$ , the probability of lock is simply the ratio of the volumes of the lock area to the total two-dimensional Euclidean space  $\mathcal{R}^2$ , i.e.,  $\Pr\{\text{Lock}\} = \pi/2\pi = 0.5$ . For the case of  $|\Delta f| \neq 0$  at high  $E_s/N_0$  values, recall that  $\Pr\{\text{Lock}\}$  equals the probability that at least  $N_T$  symbols lie inside the lock area.

As a consequence of the argument above, up to  $(N - N_T)$  symbols can lie outside the lock area just before or after its boundary. The lock area angular range increases by  $\Theta_2 = (N - N_T)2\pi\Delta fT_s$ . Therefore, in the first quadrant, the normalized area of the lock region increases from  $\Theta_1 = \pi/4$  to  $\Theta_1 + \Theta_2 = \pi/4 + (N - N_T)2\pi\Delta fT_s$ . It follows that, at high  $E_s/N_0$ , the probability of lock tends to a constant value

$$\Pr\{\text{Lock}\} \rightarrow \frac{1}{2} + 4(N - N_T)\Delta fT_s. \quad (9)$$

As an example, for  $\Delta fT_s = 0.001$ ,  $N = 50$  and  $N_T = 27$ ,  $\Pr\{\text{Lock}\} \rightarrow 0.592$ . For other modulation formats, similar results can be obtained in a straight forward manner. For 16-QAM modulation, at high  $E_s/N_0$  and in the absence of frequency offset, the probability of lock, averaged over  $\phi$ , equals 0.26.

### C. Acquisition Time

The acquisition time, denoted  $T_a$ , is defined as the time period from an initial condition of the multiple-mode PLL to acquisition (lock indication). The average value of  $T_a$ , over all possible initial conditions (phases), is obtained from the lock probability  $P_o(M, \phi)$ , analyzed in the previous section, as follows:

$$T_a = \frac{1}{2\pi} \int_0^{2\pi} t_a(\phi) d\phi, \quad (10)$$

where  $\phi$  is the initial phase value, as defined in the previous section, and  $t_a(\phi)$  is the acquisition time when the initial phase is equal to  $\phi$ .

Eq. (10) is obtained by averaging  $t_a(\phi)$ , with  $\phi$  in the range  $[0, 2\pi]$ , where the value of  $t_a(\phi)$  may be expressed as follows:

$$t_a(\phi) = P_o(M, \phi) + \sum_{i=2}^{N_{max}} iP_o(M, N(i-1)\Delta\theta + \phi) \prod_{j=1}^{i-1} (1 - P_o(M, N(j-1)\Delta\theta + \phi)), \quad (11)$$

where  $N_{max} \rightarrow \infty$ . As a consequence, the correct value of  $t_a(\phi)$  cannot be evaluated directly from (11). However, it is still possible to get a very good approximation by upper bounding the maximum value of  $t_a(\phi)$ . In the results reported in this section, a maximum value of  $T_a(\phi) = 200$  was used.

Simulation results and theoretical expressions on the mean acquisition time are shown in Figs. 2 to 5. In the figures, the

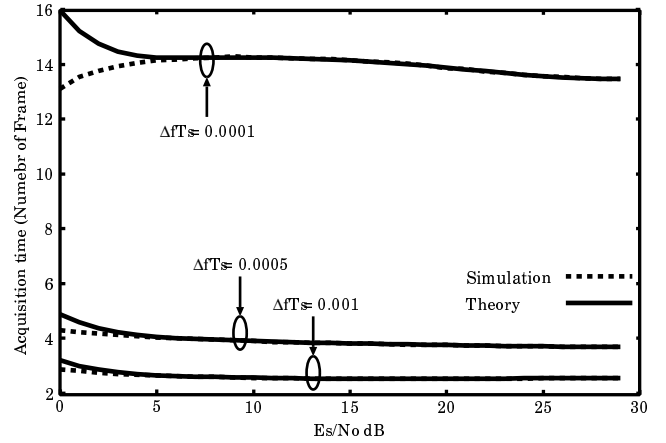


Fig. 2. Acquisition time vs  $E_s/N_0$  in BPSK,  $\Delta fT_s = 0.0001, 0.0005, 0.001$

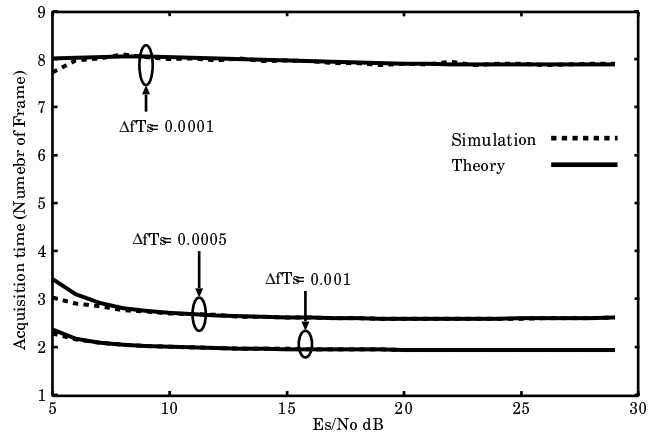


Fig. 3. Acquisition time vs  $E_s/N_0$  in QPSK,  $\Delta fT_s = 0.0001, 0.0005, 0.001$

mean acquisition time is reported in number of frames, with each frame equal to 50 symbols. Notice that the theoretical and simulation values are very close in the high  $E_s/N_0$  region. On the other hand, in the low  $E_s/N_0$  region, a certain gap between theory and simulation is present. In the case of small  $\Delta fT_s$ , the acquisition time increases as opposed to the case of larger  $\Delta fT_s$ .

These results confirm numerically the fact that if the initial position of a received symbol is far from the lock area, and the normalized frequency offset  $\Delta fT_s$  is relatively small, then the acquisition time is large.

For both phase and carrier offset equal to zero, the lock probabilities of the modulation schemes considered in this paper are shown in Fig. 6. This allows to compare directly the performance of the proposed scheme with that of other conventional approaches to modulation identification. In particular, the probability of lock detection and modulation identification for 16-QAM modulation, shown in Fig. 6, compares very favorably with the results reported in Fig. 2 of [1], when considering that

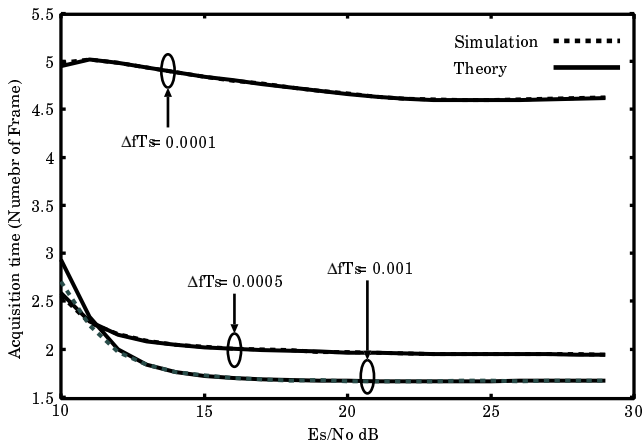


Fig. 4. Acquisition time vs Es/No in 8PSK,  $\Delta fT_s = 0.0001, 0.0005, 0.001$

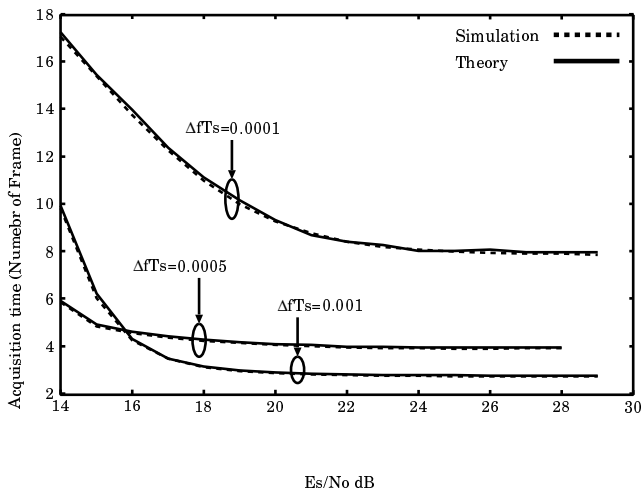


Fig. 5. Acquisition time vs Es/No in 16QAM,  $\Delta fT_s = 0.0001, 0.0005, 0.001$

a short observation interval of 50 symbols was used to obtain the results in this paper.

#### IV. CONCLUSIONS

A non-data-aided carrier recovery technique for multiple modulation formats was introduced. A digital PLL, in conjunction with a bank of phase lock detectors, is utilized in the proposal. The specific phase error detector used in the carrier recovery loop is selected based on the output of a modulation identification logic, which is designed not only to recognize a given modulation scheme, but also to avoid false locks and incorrect identification in the presence of static phase/frequency offsets. This is achieved with additional sector counters and an augmented identification logic.

A theoretical analysis was presented for the probability of lock detection and the mean acquisition time. These results were confirmed by Monte Carlo simulations. It was found that when noise conditions are such that phase lock is possible, the theo-

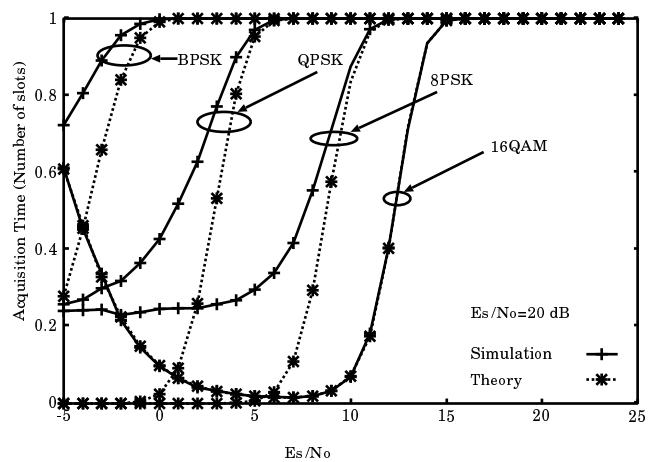


Fig. 6. Lock probability vs Es/No, initial phase offset and carrier offset is zero

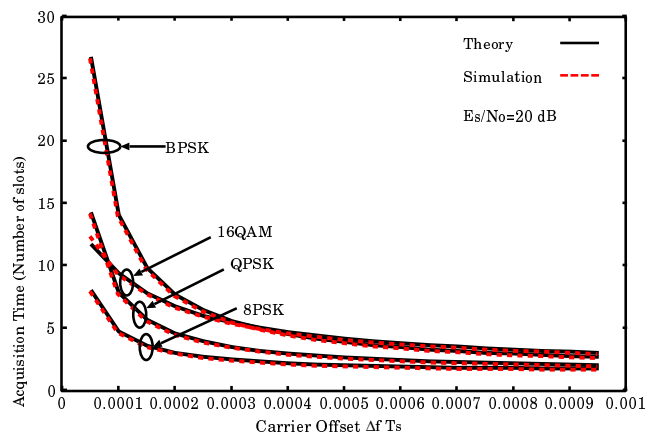


Fig. 7. Acquisition time vs Carrier offset, Es/No=20dB

retical results closely match the simulations. The simplicity and good performance of the proposed method are evident. Extensions of the results presented in this paper to imperfect timing recovery, as well as to residual intersymbol interference caused by multipath fading channel conditions, remain topics of future research.

#### REFERENCES

- [1] A. Swami and B.M. Sadler, "Hierarchical Digital Modulation Classification Using Cumulants," *IEEE Trans. Comm.*, vol. 48, no. 3, pp. 416-429, March 2000.
- [2] H. Meyr, M. Moeneclaey and S.A. Fechtel, *Digital Communication Receivers*, Wiley, 1998.
- [3] R.H. Morelos-Zaragoza, "Joint Phase-Lock Detection and Identification of M-PSK/M-QAM Modulation," *Proc. 2000 Third Generation Wireless Communications Conference (3GWireless'00)*, pp. 272-279, San Francisco, CA, June 15, 2000.
- [4] R.H. Morelos-Zaragoza, Kenta Umabayashi "Adaptive Carrier Recovery with Modulation Identification Joint Phase-Lock Detection and Identification of M-PSK/M-QAM Modulation," *Proc. 2001 International Symposium on Signals, Systems, and Electronics (ISSSE'01)*, pp. 216-219, Tokyo, July 26, 2001.